MOLECULAR AND CELLULAR BIOLOGY, Sept. 2005, p. 7637–7644 Vol. 25, No. 17
0270-7306/05/$08.00+0 doi:10.1128/MCB.25.17.7637–7644.2005

The Nuclear Form of Phospholipid Hydroperoxide Glutathione Peroxidase Is a Protein Thiol Peroxidase Contributing to Sperm Chromatin Stability

M. Conrad,[1,2]* S. G. Moreno,[1,3] F. Sinowatz,[4] F. Ursini,[5] S. Kölle,[4] A. Roveri,[5] M. Brielmeier,[2] W. Wurst,[6] M. Maiorino,[5] and G. W. Bornkamm[1]

Institute of Clinical Molecular Biology and Tumour Genetics, GSF Research Centre for Environment and Health, Marchioninistr. 25, D-81377 Munich, Germany[1]; Department of Comparative Medicine, GSF Research Centre for Environment and Health, Ingolstädter Landstr. 1, D-85764 Neuherberg, Germany[2]; UMR Gamétogenèse et Génotoxicité, CEA, INSERM U566, Université Paris 7, F-92265 Fontenay-aux-Roses, France[3]; Department of Veterinary Anatomy II, Ludwig-Maximilian University of Munich, Veterinärstraße 13, D-80539 Munich, Germany[4]; Department of Biological Chemistry, University of Padova, Viale G. Colombo, 3, I-35121 Padova, Italy[5]; and Institute of Developmental Genetics, GSF Research Centre for Environment and Health, Ingolstädter Landstr. 1, D-85764 Neuherberg, Germany[6]

Received 20 January 2005/Returned for modification 5 April 2005/Accepted 7 June 2005

The selenoenzyme phospholipid hydroperoxide glutathione peroxidase (PHGPx) is regarded as the major molecular target of selenodeficiency in rodents, accounting for most of the histopathological and structural abnormalities of testicular tissue and male germ cells. PHGPx exists as a cytosolic form, mitochondrial form, and nuclear form (nPHGPx) predominantly expressed in late spermatids and spermatozoa. Here, we demonstrate that mice with a targeted deletion of the *nPHGPx* gene were, unlike mice with the full knockout (KO) of *PHGPx*, not only viable but also, surprisingly, fully fertile. While both morphological analysis of testis and epididymis and sperm parameter measurements did not show any apparent abnormality, toluidine blue and acridine orange stainings of spermatozoa indicated defective chromatin condensation in the KO sperm isolated from the caput epididymis. Furthermore, upon drying and hydrating, KO sperm exhibited a significant proportion of morphologically abnormal heads. Monobromobimane labeling and protein-free thiol titration revealed significantly less extensive oxidation in the cauda epididymis when compared to that in the wild type. We conclude that nPHGPx, by acting as a protein thiol peroxidase in vivo, contributes to the structural stability of sperm chromatin.

Sperm chromatin condensation during the final steps of spermatogenesis in mammals is a multistep process that includes the sequential replacement of the majority of histones by transition proteins and protamines in testis (6, 7). During epididymal transit of spermatozoa, protamine thiol oxidation is completed and intra- and intermolecular cross-links are formed. Hence, a transcriptionally inactive and tightly packed haploid genome is generated rendering sperm nuclei more resistant to mechanical and chemical insults (2). Recently, Cho and colleagues showed that chimeric mice hemizygous for protamine 1 or 2 fail to transmit the targeted allele to the germ line (8).

Selenium depletion studies of rodents clearly demonstrated the importance of this trace element in male fertility. Third generation selenium deficiency is associated with structural abnormalities, such as broken midpieces of sperm tails, giant heads, and reversible testicular atrophy (5, 34). Due to its particular high expression in mammalian testis (21) and its resistance to selenium deprivation in testis, the selenoenzyme phospholipid hydroperoxide glutathione peroxidase (PHGPx) is thought to account for most of the defects associated with severe selenium deficiency.

PHGPx was initially characterized as a lipid peroxidation-inhibiting protein (33) and was later shown to be an unusual member of the glutathione peroxidase family, in particular for its scarce specificity for both the oxidizing and reducing substrates (32). Most relevant in this respect was the observation that, in the presence of low glutathione (GSH) concentration, specific protein –SH groups may act as a reductant in the catalytic cycle with a stoichiometry of 2 equivalents of thiol per mole of hydroperoxide (13, 22, 28, 31). Apparently due to this reaction, during spermatogenesis, PHGPx behaves as a soluble peroxidase as long as GSH levels are high; however, due to the drop of GSH levels (29), PHGPx becomes enzymatically inactive and results in a cross-linked, insoluble protein representing the major structural constituent of the mitochondrial sheath of the midpiece of mature spermatozoa (31).

Three different transcripts of PHGPx exist, differing in their 5′ extension and coding for a cytosolic protein, mitochondrial protein, and nuclear protein (24, 25). The latter was recently identified as a sperm nucleus-specific 34-kDa selenoprotein (nPHGPx; also called snGPx, for sperm nucleus-specific glutathione peroxidase) (24).

* Corresponding author. Mailing address: Institute of Clinical Molecular Biology and Tumour Genetics, GSF Research Centre for Environment and Health, Marchioninistr. 25, D-81377 Munich, Germany. Phone: 49-89-7099525. Fax: 49-89-7099500. E-mail: marcus.conrad@gsf.de.

The *nPHGPx* gene shares all exons except the first with the cytosolic and mitochondrial forms of PHGPx. Alternative first exon (Ea) usage, and not alternative splicing, was shown to be responsible for the generation of the mRNA encoding nPHGPx (20, 23). This Ea of *nPHGPx* encodes both a nuclear import signal and clusters rich in arginine and lysine residues, reminiscent of protamines (24). Circumstantial evidence suggested a crucial role for nPHGPx in sperm chromatin condensation: its nuclear localization, the coincidence in the spatial and temporal expression with protamines, its structural similarity to protamines, its in vitro documented thiol peroxidase activity, and the presence of improper condensed giant cells in sperm specimens from selenium-depleted rodents. We hypothesized that nPHGPx may bind via its highly basic N terminus to sperm chromatin and may introduce disulfide bridges into protamines in order to achieve a tight package of the male haploid genome. To prove this hypothesis, we generated mice specifically lacking nPHGPx.

MATERIALS AND METHODS

Generation of *nPHGPx* KO mice. An AflII/NarI (NarI site blunt ended) fragment isolated from vector pMC42, which carries an 18-kbp fragment including the murine PHGPx locus, was inserted in pBluescript SK+ (Stratagene Inc., La Jolla, CA) digested with AccI and XbaI (blunt ended) in order to obtain pMC69. By PCR cloning, a replacement cassette was amplified containing a 5′ NotI site, a characteristic EcoRV site, the enhanced green fluorescent protein (*EGFP*) gene followed by a translational STOP element in every possible reading frame, and a characteristic AseI site (EaGFPkoforw1/EaGFPkorev1, 5′-TGCG GCCGCCGATATCGTGAGCAAGGGCGAGGAGCTGTTC-3′/5′-TAGTAC TGGATTAATTAGTTATCTAGATCCGGTGGATCTG-3′) (Fig. 1A). This cassette was inserted in pMC69 (NotI/ScaI), thereby replacing the main part of Ea (pMC70). A NotI fragment including the in-frame *EGFP* cassette replaced parts of the 5′ homologous arm of pPNT4.8 (unpublished), a targeting vector derived from pPNT4 (9) that already harbored both homologous arms required for gene targeting (pPNT4.9). Gene targeting in embryonic stem (ES) cells was carried out as described previously (15). DNA of 500 ES cell clones digested with EcoRV was screened for homologous recombination by Southern blotting with a 3′ external probe. Random integration was excluded with a probe specific for neomycin phosphotransferase. Positive ES cell clones arose at a frequency of 1%. Three ES cell clones were microinjected into C57BL/6J blastocysts, and all three ES cell clones generated chimera that finally transmitted the *nPHGPx* knockout (KO) allele to the germ line. To facilitate genotyping of *nPHGPx* KO mice, two primer pairs were used: one specific for the wild-type (WT) (I1f2/Earev1, 5′-T CGGCGGCGCCTTGGCTACCGGCTC-3′/5′GGATCCGCCGCGCTGTCTG CAGCGTCCC-3′) and one specific for the KO (I1f2/eGFPrev, 5′-TGAAGAA GTCGTGCTGCTTCATGTGG-3′) allele.

RNA isolation and semiquantitative RT-PCR. Isolation of testis RNA, DNase treatment, and reverse transcription (RT) were carried out as described previously (23). Primer pairs specific for the aldolase gene (Aldolase1/2, 5′AGCTGTCTGACATCGCTCACCG-3′/5′-CACATACTGGCAGCGCTTCA AG-3′), the GAPDH gene (GAPDH1/2, 5′-CTCACTCAAGATTGTCAGCAA TG-3′/5′-GAGGGAGATGCTCAGTGTTGG-3′), and the mitochondrial form of *PHGPx* (P32/E2rev1, 5′-GCAAGCCATACTCGGCCTCGCGCGTCC-3′/5′-CCAGGCAGACCATGTGCCCGTCGATGTCC-3′), as well as one for the deleted region of the alternative exon (Eaforw2, 5′-CTCGCCGGATGGAGCCC ATTCC-3′/E2rev1) were used.

In situ hybridization. The corresponding region of the deleted part of Ea of the *PHGPx* gene was amplified by PCR using pMC42 as a template (forward/reverse primer, 5′-GGGACGCTGCAGACAGCGCGGCGGATCC-3′/5′-ACT GGGGAGGCTCTTGCAGCAGAGG-3′) and cloned in pDrive (QIAGEN, Hilden, Germany). Generation of digoxigenin-labeled RNA probes and in situ hybridization were performed as described previously (23).

Biological samples. Spermatozoa, obtained from approximately 12-week-old mice, were consistently prepared from caput and cauda epididymis and vas deferens by gentle squeezing in cold phosphate-buffered saline (PBS). After passing through a 100-μm mesh filter, the cell suspension was centrifuged at 600 × *g* for 10 min and washed twice with 10 ml of the same buffer. Sonication-resistant nuclei from testis were prepared according to reference 24.

Western blotting. Pelleted sperm were dissolved in 0.1 M Tris-HCl, pH 7.8, buffer containing 0.1% (vol/vol) Triton X-100, 0.1 M 2-mercaptoethanol, and 6 mM guanidine-HCl, which was replaced by Laemmli buffer using Micro Biospin P6 cartridges (Bio-Rad, München, Germany). Gel electrophoresis was performed according to reference 18. Sodium dodecyl sulfate (SDS)-polyacrylamide gel electrophoresis-separated proteins (10 μg each) were blotted onto a nitrocellulose membrane in 3-[cyclohexylamino]-1-propanesulfonic acid (CAPS)-NaOH (0.01 M), 10% methanol, pH 11, and probed with a PHGPx-specific antibody at a dilution of 1:1,000 (27). Detection was achieved by incubation with biotinylated anti-rabbit immunoglobulin G and streptavidin-alkaline phosphatase complex.

Hematoxylin-eosin histology of testis and epididymis. Freshly dissected tissues were immediately fixed in Bouin's solution or in 4% (wt/vol) paraformaldehyde in PBS at 4°C overnight, embedded in paraffin, and cut in 5-μm-thick sections. Sections were deparaffinized in xylol, hydrated in graded ethanol series, stained with Mayer's hematoxylin (Sigma, Taufkirchen, Germany) for 5 min, washed in water, briefly treated with 1% acid ethanol, washed again, and stained with 1% eosin Y (Merck, Darmstadt, Germany) for 3 min. Then the sections were washed again in water, dehydrated in graded ethanol series, treated with xylol, and mounted.

Ultrastructural analysis. (i) SEM. Sperm were washed twice in Soerensen buffer, pH 7.4 (1:5 solution of 0.07 M KH_2PO_4 and 0.07 M Na_2HPO_4-$2H_2O$), fixed in 1% glutaraldehyde in Soerensen buffer at 4°C for 24 h, washed again, and centrifuged onto slides coated with 3-aminopropylene-ethoxysilane. Then sperm were dehydrated in an ascending series of acetone (10%, 20%, 30%, 40%, 50%, and 60% twice for 5 min each; 70%, 80%, and 90% for 1 h each; 100% for 12 h) and dried in a Union Point dryer CPD 030 (Bal-Tec, Walluf, Germany) using liquid CO_2 as the transitional fluid. Dried sperm were coated with 12-nm gold-palladium by a Union SCD 040 sputtering device (Bal-Tec). Scanning electron microscopy (SEM) observations were made with the Zeiss scanning electron microscope DSM 950 using magnifications of ×200 to ×10,000 (Carl Zeiss, Jena, Germany).

(ii) Transmission electron microscopy. Transmission electron microscopy for ultrastructural analyses of testis and epididymis was principally carried out as described in reference 10.

ISEL and immunohistochemistry. The in situ end-labeling (ISEL) method and immunohistochemistry tests were performed as follows. Detection of apoptotic cells and proliferating cellular nuclear antigen (PCNA) staining were carried out as described previously (10). The latter protocol was also applied for 8-hydroxyguanosine staining of paraffin-embedded sections after boiling sections twice in 10 mM sodium citrate buffer for antigen retrieval (30). Anti-8-hydroxyguanosine was the primary antibody (QED Bioscience Inc., San Diego, CA); the secondary antibody was an anti-mouse biotinylated antibody, BA-2000 (Vector Laboratories Inc.).

Sperm parameter analysis. Spermatozoa were collected from the cauda epididymis. Their concentration, motility, and progressivity were estimated by using the Integrated Visual Optical System (IVOS) for sperm analysis according to the manufacturer's recommendation (Hamilton Thorne Research, Beverly, MA).

TB and AO staining (modified Rigler-Roschlau method). Both the toluidine blue (TB) and acrid orange (AO) methods were performed with fresh sperm smears as reported recently (12). In brief, sperm were fixed in 96% ethanol-acetone (1:1) for 30 min at 4°C, denatured in 0.1 N HCl at 4°C for 5 min, washed in distilled water, and stained with 0.05% TB in McIlvain buffer (200 mM Na_2HPO_4, 100 mM citric acid, pH 3.5) for 10 min at room temperature. Slides were dehydrated in butanol at 37°C and embedded in Roth medium (Roth GmbH, Karlsruhe, Germany). For AO staining, sperm were fixed in 96% ethanol-acetone (1:1) at 4°C for 30 min, rehydrated in a graded ethanol series at room temperature, washed in PBS, treated with 1 N HCl for 1 min at 60°C, and rinsed three times in distilled water. Slides were dipped into McIlvain buffer for 5 min, stained with freshly prepared AO (0.1 mM), and subsequently rinsed three times for 5 min each with AO (0.001 mM) in the same buffer. Sperm were immediately evaluated by fluorescence microscopy.

Sperm chromatin decondensation assay with SDS. Prior to decondensation, reactive thiols were blocked by incubating isolated sperm in 10 mM *N*-ethylmaleimide (Sigma, Taufkirchen, Germany) in PBS for 30 min at 37°C with gentle shaking. Subsequently, sperm were washed in PBS, incubated in 0.5% SDS, 50 mM Tris-HCl, pH 7.5, for 20 min at 37°C with gentle shaking, stained with ethidium bromide, and immediately evaluated by fluorescence microscopy (Axioplan; Carl Zeiss, Oberkochen, Germany).

Protein thiol measurement. A stock solution of 50 mM monobromobimane (mBrB [Thiolyte]; Calbiochem, Schwalbach, Germany) was prepared in 100% acetonitrile and stored at 4°C in the dark for up to 1 month. This was diluted to 1 mM with PBS and added to spermatozoa resuspended in PBS at a final

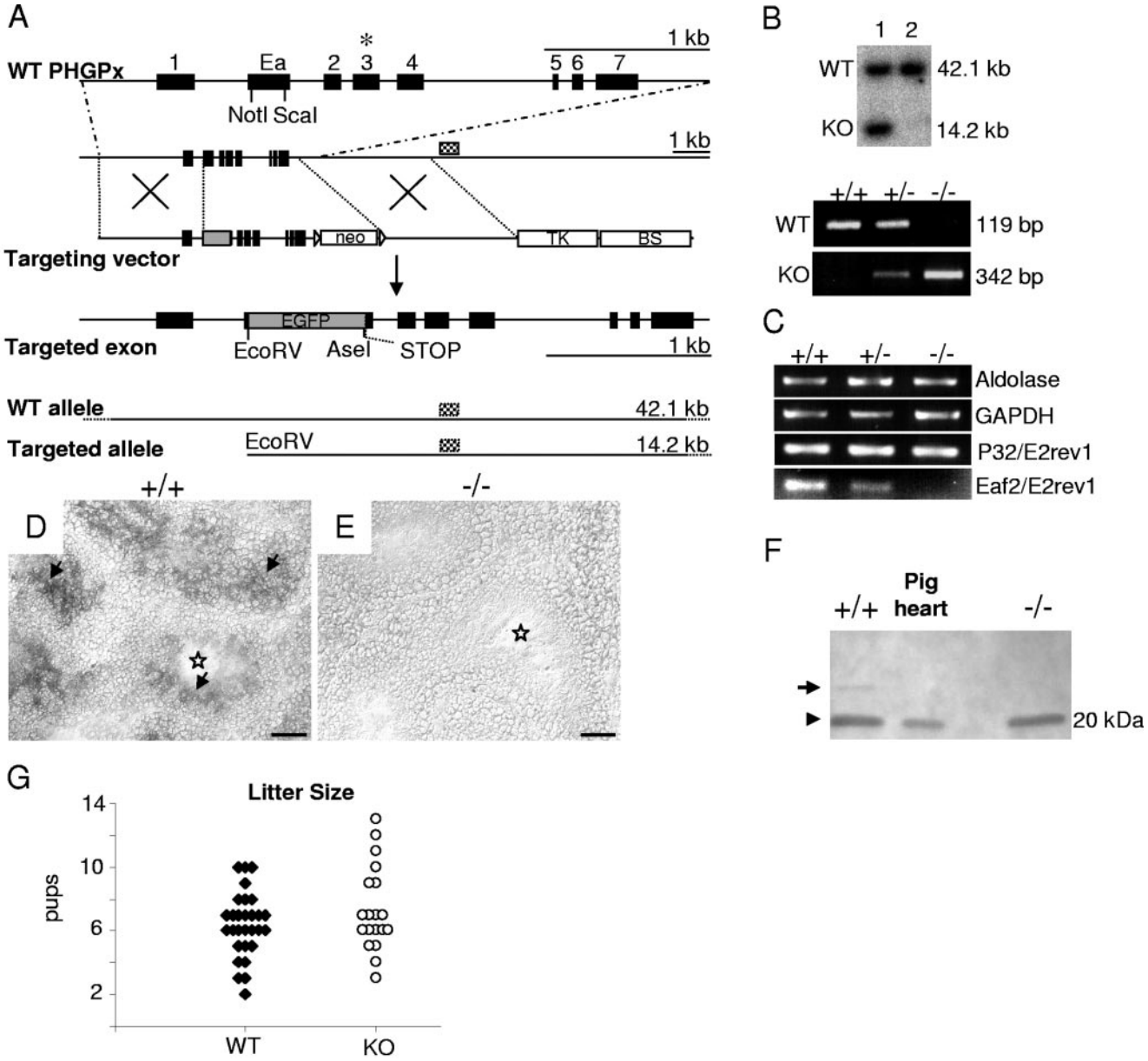

FIG. 1. Gene targeting of *nPHGPx* in mice. (A) Strategy for disruption of the nuclear form of *PHGPx*. WT *PHGPx* is shown in the upper line; localization of the selenocysteine codon UGA is marked with an asterisk. To specifically delete *nPHGPx*, most of the coding region of Ea was replaced by the *EGFP* gene. A translational STOP cassette was inserted 3′ of *EGFP*. For negative selection of transfected ES cells, the thymidine kinase gene (TK) was placed downstream from the 3′ arm. Underneath, expected DNA fragments, resulting from a characteristic restriction digest with EcoRV and detection with a 3′ external probe (checkered rectangles), are depicted (neo, neomycin phosphotransferase gene; BS, pBluescript SK+ backbone). (B) Verification of homologous recombination in ES cell clones (lane 1) by Southern blotting. Below, germ line transmission of the targeted allele and genotyping of offspring obtained from heterozygous intercrosses by two PCRs, one specific for the WT and one specific for the KO allele. (C) Semiquantitative RT-PCR analyses of testis mRNA. (D and E) In situ hybridization of testis sections confirmed the absence of the targeted region in KO testis (E). Arrows point at *nPHGPx* expression around the luminal face of WT germinal epithelium (D). Stars indicate the lumen of tubuli seminiferi. (F) Western blotting of testis extracts revealed low levels of the longer truncated product of nPHGPx (25.9 kDa) in WT tissue (arrow), which is absent in KO tissue. Protein levels of cytosolic/mitochondrial forms of PHGPx (20 kDa) are equal in WT and KO tissue. Cytosolic extracts from pig heart served as a positive control. (G) No difference in litter sizes between WT ($n = 30$ litter) and KO ($n = 20$ litter) mice. Bars = 50 μm (D and E).

concentration of 20×10^6 cells/ml. After labeling at room temperature for 30 min in the dark, spermatozoa were twice washed with PBS. To solubilize labeled proteins, spermatozoa were dissolved in 0.1 M Tris-HCl, pH 7.8, containing 0.1% (vol/vol) Triton X-100, 0.1 M 2-mercaptoethanol, and 6 mM guanidine-HCl. Proteins were precipitated in 4% (wt/vol) trichloroacetic acid and washed with cold ethanol. Final solubilization was achieved in 10 mM NH_4HCO_3, pH 8.3, containing 1% (wt/vol) SDS. Fluorescence emission was measured by a RF-5000 spectrofluorophotometer (Shimadzu) with excitation and emission wavelengths of 380 and 470 nm, respectively. Total thiol content was measured by repeating the labeling procedure after the solubilization and reduction step.

Ex vivo labeling of spermatozoa. Spermatozoa were resuspended in 0.5 ml PBS, labeled with a solution of 1 mM mBrB prepared as described above, washed

twice with PBS, and resuspended in a minimal volume of PBS prior to fluorescence microscopy evaluation (Axioplan; Carl Zeiss) (excitation and emission wavelengths of 365 to 395 and 420 nm, respectively).

RESULTS

Generation of nPHGPx KO mice. The *PHGPx* gene is composed of 8 exons spanning a region of approximately 3 kbp. The mRNAs encoding the mitochondrial (*mPHGPx*) and cytosolic (*cPHGPx*) forms of PHGPx are initiated at alternative transcription initiation sites (16, 25) and share exons 1 to 7 but exclude Ea localized between exons 1 and 2 (Fig. 1A). In contrast, nPHGPx lacks the first exon and consists of exons Ea and 2 to 7 (23, 24). The Ea encodes both a nuclear localization signal and clusters rich in arginine and lysine, most likely required for binding of nPHGPx to DNA. Since loss of the whole *PHGPx* gene or of exons Ea to 7 is associated with early embryonic lethality in mice (14, 36), we replaced large parts of the coding region of Ea with *EGFP*, generating a fusion gene consisting of the six N-terminal amino acids of nPHGPx (MGRAAA) and EGFP. Its functionality was controlled by transient overexpression of the fusion protein in HeLa and NIH 3T3 cells under the control of the human cytomegalovirus promoter. Strong cytoplasmic staining of the cells could be observed (data not shown); however, unfortunately this fusion protein was not functional in vivo, meaning we could detect neither green spermatozoa nor green fluorescing testicular tissue. The *EGFP* gene was flanked by characteristic restriction sites for confirmation of homologous recombination of the targeting construct in ES cells. Additionally, a translational STOP cassette was inserted in every possible reading frame 5′ of the fusion gene. The remaining 3′ coding region of Ea, corresponding to 11 amino acids, did not contain any translational START codon. Hence, our strategy aimed at removing the coding region of Ea, thereby abolishing *nPHGPx* expression without affecting *mPHGPx* and *cPHGPx* expression.

The construct for targeting *nPHGPx* in ES cells, a Southern blot demonstrating germ line transmission of the targeted allele, and genotyping of tail DNA are shown in Fig. 1B. Intercross of $nPHGPx^{+/-}$ mice produced viable $nPHGPx^{-/-}$ mice. Of 191 offspring from heterozygous breeding pairs, 22.5% were WT and 52.4% were heterozygous and 25.1% homozygous KO for *nPHGPx*. Thus, we conclude that nPHGPx is not essential for embryonic development and survival. Semiquantitative RT-PCR analysis with testis mRNA was used to verify the absence of the coding region of Ea. Primer pair P32/E2rev1 was used to detect the mitochondrial form of *PHGPx*. No differences in *mPHGPx* mRNA levels were noticeable in mice of the different genotypes (Fig. 1C). However, when the primer Eaforw2, specific for the deleted part of Ea, was used in combination with E2rev1, a clear reduction of *nPHGPx* mRNA levels in $nPHGPx^{+/-}$ and absence in *nPHGPx* KO mice could be demonstrated. We confirmed our RT-PCR data by in situ hybridization experiments on testis sections using an antisense probe specific for the deleted region of Ea (Fig. 1D and E). No specific signal could be detected in sections from $nPHGPx^{-/-}$ mice (Fig. 1E). In contrast, a clear signal especially around the luminal face of tubuli seminiferi was noticed in WT mice (Fig. 1D), which is in accordance with previous findings (20, 23). Furthermore, the absence of the 25.9-kDa immunoreactive band, representing the principal form of nPHGPx in late spermatids and spermatozoon heads (19), confirmed that nPHGPx is not expressed in the testes (Fig. 1F) and spermatozoa (data not shown) of KO mice.

Fertility of *nPHGPx* KO mice. We assumed a crucial role for nPHGPx in sperm chromatin condensation, and to test this hypothesis, breedings of male $nPHGPx^{-/-}$ mice with C57BL/6 mice were performed. To our surprise, male $nPHGPx^{-/-}$ mice were fully fertile and litter sizes (Fig. 1G) (6.4 ± 2.0 pups [$n = 30$] versus 7.3 ± 2.7 pups [$n = 20$], control versus KO, respectively) and whelping intervals (30.4 ± 13.0 days [$n = 19$] versus 30.5 ± 8.3 days [$n = 11$], control versus KO, respectively) were indistinguishable from those of their WT counterparts.

Morphological analyses of germinal epithelium and germ cells. Histological examinations of testis and epididymal tissue did not show any differences between $nPHGPx^{+/+}$, $nPHGPx^{+/-}$, and $nPHGPx^{-/-}$ siblings (Fig. 2, A to D). Likewise, SEM of isolated epididymal spermatozoa and ultrastructural analysis of testis and epididymis did not reveal any obvious differences between WT and KO mice (Fig. 2E to K) (data not shown). Staining with PCNA and ISEL staining was performed to test whether proliferation of spermatogonia or apoptosis of spermatogenic cells was affected by loss of *nPHGPx*. We could not detect any differences in WT and heterozygous and homozygous KO mice (data not shown). Since PHGPx is known to have antioxidant properties, we stained testis sections with an antibody recognizing 8-hydroxy-deoxyguanine. Again, no signs of increased DNA damage of germ cells could be observed (data not shown).

Sperm parameters. Sperm parameters such as concentration, motility, and progressivity of spermatozoa isolated from the cauda epididymis were determined by using the IVOS. Similar to the histological findings described above, we could not find any difference in the analyzed sperm parameters of mice of any genotype, supporting the notion that male *nPHGPx* KO mice are fully fertile (Fig. 3A) (data not shown).

Sperm chromatin condensation. We used TB and AO staining to study the integrity of sperm chromatin (12). Protamine cross-linking by formation of intra- and intermolecular disulfide bonds is considered to render sperm chromatin resistant to mechanical and chemical insults. Thus, susceptibility to denaturation of chromatin by heat or acid can be used to monitor protamine cross-linking. Upon acidic or heat treatment of sperm DNA, green/yellow fluorescent AO staining indicates fully condensed, nondenatured double-stranded DNA, whereas red fluorescence indicates noncondensed partially single-stranded DNA. TB staining follows the same principle, where pale blue staining and violet/dark blue staining visualize normal and incomplete sperm chromatin condensation, respectively.

Spermatozoa were consistently isolated from the caput and from the cauda epididymis and subjected to both staining techniques (Fig. 3B to L). A clear difference in TB staining was observed only in spermatozoa derived from the caput epididymis. Approximately half of KO spermatozoa showed dark blue TB staining as compared to 8% in WT spermatozoa (Fig. 3B, C, and F). No such difference could be observed in spermatozoa isolated from the cauda epididymis (Fig. 3D to F). AO staining confirmed the results obtained by TB staining (Fig. 3G to L). Of note, when we prepared smears of sperma-

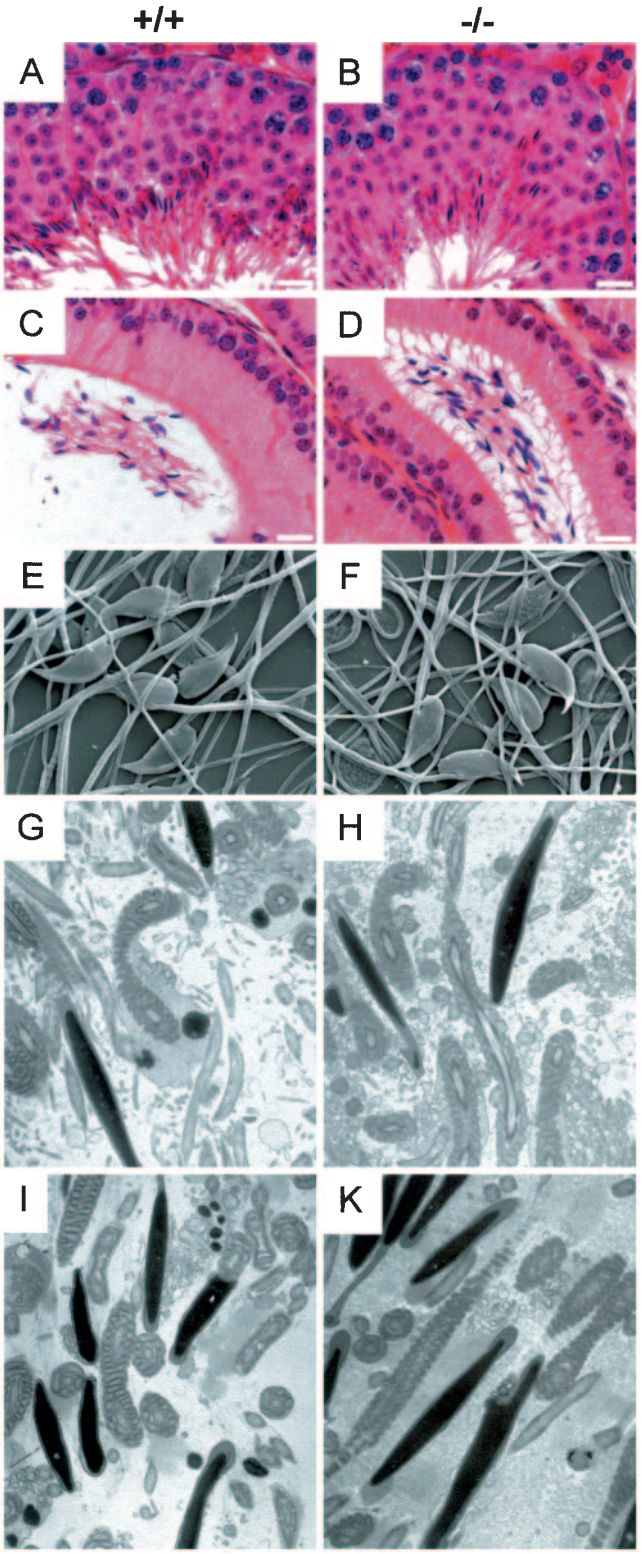

FIG. 2. Histological analyses of testis and epididymis. (A to D) Hematoxylin-and-eosin staining of testis (A and B) and epididymis sections (C and D) did not show any gross abnormalities in KO (n = 8) (B and D) as compared to WT (n = 8) (A and C) tissue. Shown are scanning electron microscopy of spermatozoa isolated from the cauda epididymis (E and F) (n = 2 each) and ultrastructural analysis of sperm derived from the caput (G and H) (n = 2 each) or cauda (I and K) (n = 2 each) epididymis. Bars = 10 μm.

tozoa, let them dry without fixation, and hydrated them with phosphate-buffered saline, around one-fourth of KO spermatozoa displayed morphologically abnormal sperm heads (Fig. 3M to O). Again, this was only apparent in spermatozoa isolated from the caput epididymis of KO mice. Additionally, spermatozoa were exposed to 0.5% SDS in order to assess the structural stability of sperm nuclei (Fig. 3P to T). Similarly to the TB and AO methods, more than half of KO sperm collected from the caput epididymis displayed strongly decondensed nuclei (Fig. 3Q). This difference was again restricted to the caput epididymis. This strengthens the observation that KO sperm derived from the caput epididymis are structurally less stable than WT sperm.

Thiol content of isolated spermatozoa. With the *nPHGPx* KO model at hand, we were able to test the long-standing hypothesis that PHGPx can act as a protein thiol peroxidase in vivo. We quantified the protein thiol content of isolated spermatozoa by using the mBrB labeling technique (17) (Fig. 4). In testis and caput epididymis, no difference in the ratio of free thiols versus total thiols could be observed in spermatids and spermatozoa, respectively (Fig. 4A, C, and E). In WT spermatozoa, a strong decrease of free thiols was found along the epididymis, from more than 80% free thiols in testis to around 50% and 10% free thiols in caput and cauda, respectively (Fig. 4E), similar to the findings described for rat spermatozoa (29). However, this did not apply for KO spermatozoa, where significantly higher levels of free protein thiols were observed in KO spermatozoa obtained from the cauda epididymis. Microscopic evaluation revealed that the difference in fluorescence intensity was largely restricted to the head region in sperm from cauda epididymis and was not evident in the midpieces and tails of spermatozoa (Fig. 4A to D).

DISCUSSION

To investigate the physiological role of nPHGPx, in particular during male gametogenesis, mice with a specific deletion of the *nPHGPx* were established. Furthermore, with this model at hand, we aimed at providing an answer to the question whether nPHGPx is able to accept electrons from thiol groups other than that of glutathione in vivo. Due to early embryonic lethality of *PHGPx* KO mice (14, 36), we specifically deleted the alternative exon. Since *nPHGPx* is independently expressed from the cytosolic and mitochondrial forms of PHGPx (20, 23), we did not expect any adverse impact of the KO on expression of the cytosolic and mitochondrial forms of PHGPx. This was indeed the case, thus confirming the previously reported mechanism of *PHGPx* expression. Most surprisingly, *nPHGPx* KO mice are fertile and litter sizes are indistinguishable between WT and heterozygous and homozygous KO mice. This is also in line with histological and ultrastructural examination of testis and spermatozoa, which did not reveal any morphological abnormalities (see Fig. 2).

Though *nPHGPx* KO mice are fully fertile, we were still interested in whether nPHGPx is involved in protamine cross-linking. During epididymal transit, mammalian sperm protamines are extensively cross-linked by inter- and intramolecular disulfide bridges up to a variable extent, which is generally species specific (1, 3, 26, 29). (n)PHGPx has been proposed as the prime catalyst involved in this oxidation process, due to its

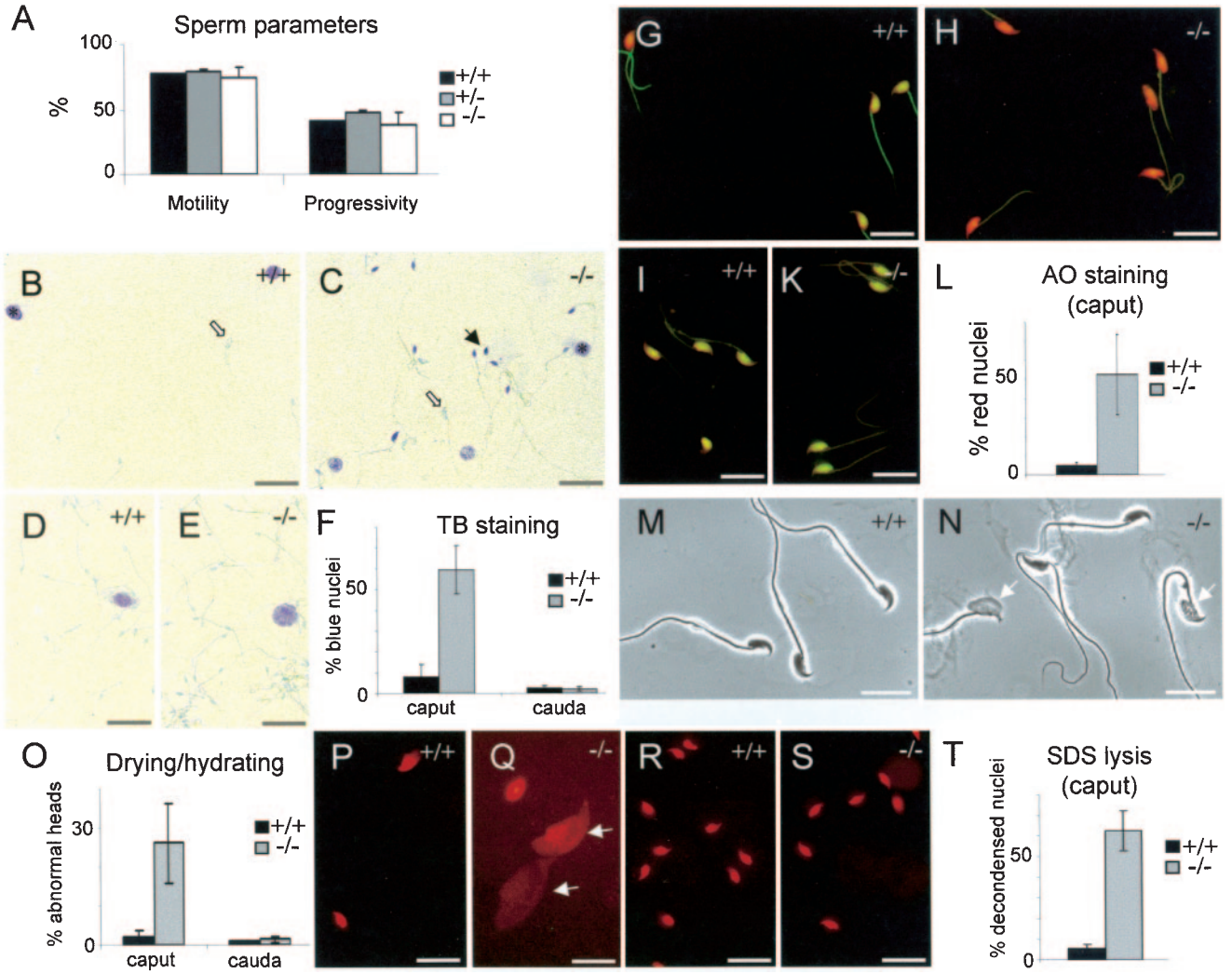

FIG. 3. Sperm parameters and TB and AO staining of spermatozoa. (A) No difference in motility and progressivity of spermatozoa of either genotype could be observed. (B to F) More than 50% of KO spermatozoa isolated from the caput epididymis showed violet-blue TB staining (black arrows in panel C) as compared to less than 10% in WT spermatozoa (B). No such difference was noticeable in spermatozoa from the caudal part of epididymis (D and E). Somatic cells are marked with an asterisk, and light blue spermatozoa are marked with open arrows. (F) Quantification of TB staining. The data are representative of two independent experiments and represent the mean ± standard deviation obtained from three control and three KO animals (n = 200 sperm each). (G to L) AO staining confirmed the results obtained from TB staining. Panels G and H show spermatozoa derived from the caput, and panels I and K show spermatazoa from the cauda epididymis. (L) Quantification of AO staining in caput. The data are representative of three independent experiments and represent the mean ± standard deviation obtained from three control and three KO animals (n = 200 sperm each). (M to O) Aberrant morphology of spermatozoa after drying and hydrating was observed in samples from caput epididymis of KO mice (arrows in panel N). (O) Quantification of these findings. The data are representative of four independent experiments and represent the mean ± standard deviation obtained from three control and three KO animals (n = 300 sperm each). (P to T) Treatment of sperm with 0.5% SDS revealed a large portion of decondensed spermatozoa (arrows in panel Q) derived from the caput epididymis of KO (Q) in contrast to WT (P) mice. (R and S) No difference was detectable in spermatozoa from the caudal part. (T) Quantification of the results obtained in panels P and Q. The data are representative of three independent experiments and represent the mean ± standard deviation obtained from four control and four KO animals (n = 200 sperm each). Bars = 10 μm.

predominance in mammalian male germ cells and its peculiar reducing substrate specificity (21, 28, 32). Thus, we applied the AO and TB staining methods to assess chromatin susceptibility to denaturation in spermatozoa isolated from caput or cauda epididymis (11, 12). Our results show that while chromatin of the WT spermatozoa entering the epididymis is already resistant to denaturation, chromatin of KO spermatozoa is more labile, reaching stability similar to that of the WT only at a later stage in the cauda (Fig. 3). This indicates that there is a phase of transient chromatin instability in caput-derived KO spermatozoa that can be unraveled by exposure to physical or chemical stress (Fig. 3). From these experiments, we conclude that chromatin condensation, albeit notably delayed, does occur in *nPHGPx* KO mice.

Since chromatin resistance to acid or heat treatment is believed to rely on the presence of disulfides in protamines, we directly addressed the issue of protein thiol redox status in spermatozoa during maturation by measuring the fluorescence

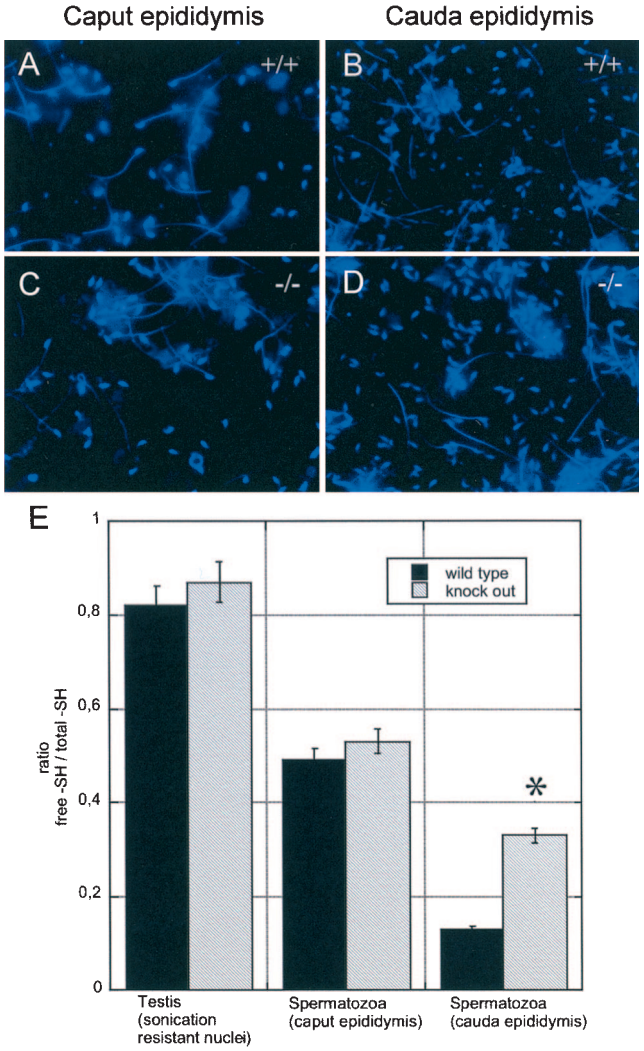

FIG. 4. Thiol-disulfide status of spermatozoa. (A to D) Microscopic evaluation of the fluorescence of spermatozoa from the caput (A and C) and cauda epididymis (B and D). No difference in fluorescence intensity could be observed in WT and KO spermatozoa from the caput epididymis (A and C), whereas less intensity was noticeable in WT spermatozoa from the cauda epididymis (B) as compared to KO spermatozoa. This difference was restricted to the head region. (E) Protein thiol status in testis sonication-resistant nuclei and spermatozoa from WT and KO mice as assessed by fluorescence photometric quantification. Significantly higher levels of free thiols were evident in KO spermatozoa. Results are expressed as a ratio between reactive –SH before and after reduction with 0.1 M β-mercaptoethanol and are representative of the mean ± standard deviation of three independent experiments (*, $P < 0.001$ versus WT).

of mBrB adducts. Our results with WT spermatozoa showed, in agreement with previous observations (29), that protein thiol oxidation is indeed a continuous process, becoming almost complete in the cauda epididymis, when approximately 90% of cysteine thiols are oxidized (Fig. 4). Surprisingly, in spermatozoa isolated from the caput epididymis, where KO chromatin was shown to be less condensed and KO sperm heads were more susceptible to dehydration-rehydration and SDS treatment, protein thiol redox status was identical to that of the WT. Significantly higher levels of free sulfhydryl groups were, however, detectable in KO spermatozoa isolated from the cauda epididymis. This indicates that (i) nPHGPx unquestionably harbors protein thiol peroxidase activity in vivo; (ii) protein thiol oxidation in sperm heads can take place also in the absence of nPHGPx, albeit with less efficiency; and (iii) at an early stage of sperm maturation when about half of the thiol groups of protamines are oxidized, the stability of sperm chromatin under denaturing conditions does not exclusively rely on the protein thiol content. In this context, one should bear in mind that oxidation is restricted not only to the head but also to the tail region of spermatozoa, although bulk oxidation occurs in the head of spermatozoa (29) (Fig. 4A and B).

The apparent discrepancy between the stability of the sperm nuclei and head with thiol redox status, occurring in the caput of epididymis, was surprising and striking. It implies that nPHGPx did already play a role in stabilizing nuclear structures in spermatozoa in the caput before and independently of protein thiol oxidation. The notion of a role for nPHGPx in structural stability is in accordance with the proposed function of PHGPx in the spermatozoon midpiece (22, 28, 31). It is conceivable that nPHGPx, already linked to DNA via its basic N terminus, becomes cross-linked to protamines via the –Se-S dead-end intermediate of the catalytic cycle, when accessible protamine thiols are limiting (22). Even very small amounts of nPHGPx covalently linked to protamines and DNA may significantly contribute to structural stability of caput sperm nuclei. Apparently, this is no longer relevant at higher oxidation levels.

The general features of nPHGPx function highlighted in this study imply that an enzyme(s) other than nPHGPx may be involved in thiol oxidation or, alternatively, that the thiol oxidation process takes place spontaneously (4). The observation that the phenotype in the head region of *nPHGPx* KO spermatozoa is much less severe than that observed under selenium deficiency strongly argues against a nonenzymatic process and for the contribution of another selenoenzyme (34). Cytoplasmic PHGPx (cPHGPx) is small enough to enter the nuclear pore by diffusion (35) and has been reported to be present in the head of spermatozoa (19). This strongly suggests that it is cPHGPx which fulfills this important function in our *nPHGPx* KO mice.

Since *nPHGPx* KO mice exhibit abnormalities at the male germ cell level not affecting fertility, we must conclude that the nuclear form of PHGPx is definitely not an indispensable player in spermatozoon physiology. Far beyond this observation, the mild phenotype, as observed in *nPHGPx* KO mice, revealed an outstanding tool to unmask the peculiar functions of PHGPx in vivo. Moreover, due to transient nuclear instability and delay in chromatin condensation, *nPHGPx* KO mice might prove an ideal model to study the susceptibility of the male genome to chemically induced mutagenesis (28a, 29a).

ACKNOWLEDGMENTS

We are most grateful to M. Krienke and A. Boersma for fruitful discussions; N. Mayr, S. Lippl, and C. Neumüller for excellent technical assistance; and P. Braghetta for advice and collaboration in fluorescence microscopy experiments.

This work was supported by the DFG-Priority Programs SPP1087 (to G.W.B., M.B., and M.C.), a fellowship from Alexander von Humboldt-Stiftung to S. Moreno, and Fonds der Chemischen Industrie and

the Italian Ministry of University and Scientific Research (grants PRIN 2002052331 to F.U. and 2003038920_002 to M.M.).

REFERENCES

1. **Balhorn, R.** 1990. Mammalian protamines: structure and molecular interactions, p. 366–395. *In* K. W. Adolf (ed.), Molecular biology of chromosome function. Springer Verlag, New York, N.Y.
2. **Balhorn, R.** 1982. A model for the structure of chromatin in mammalian sperm. J. Cell Biol. **93:**298–305.
3. **Balhorn, R., M. Corzett, J. Mazrimas, and B. Watkins.** 1991. Identification of bull protamine disulfides. Biochemistry **30:**175–181.
4. **Balhorn, R., M. Corzett, and J. A. Mazrimas.** 1992. Formation of intraprotamine disulfides in vitro. Arch. Biochem. Biophys. **296:**384–393.
5. **Behne, D., H. Weiler, and A. Kyriakopoulos.** 1996. Effects of selenium deficiency on testicular morphology and function in rats. J. Reprod. Fertil. **106:**291–297.
6. **Brewer, L., M. Corzett, and R. Balhorn.** 2002. Condensation of DNA by spermatid basic nuclear proteins. J. Biol. Chem. **277:**38895–38900.
7. **Brewer, L. R., M. Corzett, and R. Balhorn.** 1999. Protamine-induced condensation and decondensation of the same DNA molecule. Science **286:**120–123.
8. **Cho, C., W. D. Willis, E. H. Goulding, H. Jung-Ha, Y. C. Choi, N. B. Hecht, and E. M. Eddy.** 2001. Haploinsufficiency of protamine-1 or -2 causes infertility in mice. Nat. Genet. **28:**82–86.
9. **Conrad, M., M. Brielmeier, W. Wurst, and G. W. Bornkamm.** 2003. Optimized vector for conditional gene targeting in mouse embryonic stem cells. BioTechniques **34:**1136–1138, 1140.
10. **Conrad, M., C. Jakupoglu, S. G. Moreno, S. Lippl, A. Banjac, M. Schneider, H. Beck, A. K. Hatzopoulos, U. Just, F. Sinowatz, W. Schmahl, K. R. Chien, W. Wurst, G. W. Bornkamm, and M. Brielmeier.** 2004. Essential role for mitochondrial thioredoxin reductase in hematopoiesis, heart development, and heart function. Mol. Cell. Biol. **24:**9414–9423.
11. **Erenpreisa, J., T. Freivalds, H. Roach, and R. Alston.** 1997. Apoptotic cell nuclei favour aggregation and fluorescence quenching of DNA dyes. Histochem. Cell Biol. **108:**67–75.
12. **Erenpreiss, J., J. Bars, V. Lipatnikova, J. Erenpreisa, and J. Zalkalns.** 2001. Comparative study of cytochemical tests for sperm chromatin integrity. J. Androl. **22:**45–53.
13. **Godeas, C., F. Tramer, F. Micali, M. Soranzo, G. Sandri, and E. Panfili.** 1997. Distribution and possible novel role of phospholipid hydroperoxide glutathione peroxidase in rat epididymal spermatozoa. Biol. Reprod. **57:**1502–1508.
14. **Imai, H., F. Hirao, T. Sakamoto, K. Sekine, Y. Mizukura, M. Saito, T. Kitamoto, M. Hayasaka, K. Hanaoka, and Y. Nakagawa.** 2003. Early embryonic lethality caused by targeted disruption of the mouse PHGPx gene. Biochem. Biophys. Res. Commun. **305:**278–286.
15. **Joyner, A. L.** 2000. Gene targeting—a practical approach, 2nd ed. Oxford University Press, New York, N.Y.
16. **Knopp, E. A., T. L. Arndt, K. L. Eng, M. Caldwell, R. C. LeBoeuf, S. S. Deeb, and K. D. O'Brien.** 1999. Murine phospholipid hydroperoxide glutathione peroxidase: cDNA sequence, tissue expression, and mapping. Mamm. Genome **10:**601–605.
17. **Kosower, N. S., and E. M. Kosower.** 1987. Thiol labeling with bromobimanes. Methods Enzymol. **143:**76–84.
18. **Laemmli, U. K.** 1970. Cleavage of structural proteins during the assembly of the head of bacteriophage T4. Nature **227:**680–685.
19. **Maiorino, M., P. Mauri, A. Roveri, L. Benazzi, S. Toppo, V. Bosello, and F. Ursini.** 2005. Primary structure of the nuclear forms of phospholipid hydroperoxide glutathione peroxidase (PHGPx) in rat spermatozoa. FEBS Lett. **579:**667–670.
20. **Maiorino, M., M. Scapin, F. Ursini, M. Biasolo, V. Bosello, and L. Flohe.** 2003. Distinct promoters determine alternative transcription of gpx-4 into phospholipid-hydroperoxide glutathione peroxidase variants. J. Biol. Chem. **278:**34286–34290.
21. **Maiorino, M., J. B. Wissing, R. Brigelius-Flohe, F. Calabrese, A. Roveri, P. Steinert, F. Ursini, and L. Flohe.** 1998. Testosterone mediates expression of the selenoprotein PHGPx by induction of spermatogenesis and not by direct transcriptional gene activation. FASEB J. **12:**1359–1370.
22. **Mauri, P., L. Benazzi, L. Flohe, M. Maiorino, P. G. Pietta, S. Pilawa, A. Roveri, and F. Ursini.** 2003. Versatility of selenium catalysis in PHGPx unraveled by LC/ESI-MS/MS. Biol. Chem. **384:**575–588.
23. **Moreno, S. G., G. Laux, M. Brielmeier, G. W. Bornkamm, and M. Conrad.** 2003. Testis-specific expression of the nuclear form of phospholipid hydroperoxide glutathione peroxidase (PHGPx). Biol. Chem. **384:**635–643.
24. **Pfeifer, H., M. Conrad, D. Roethlein, A. Kyriakopoulos, M. Brielmeier, G. W. Bornkamm, and D. Behne.** 2001. Identification of a specific sperm nuclei selenoenzyme necessary for protamine thiol cross-linking during sperm maturation. FASEB J. **15:**1236–1238.
25. **Pushpa-Rekha, T. R., A. L. Burdsall, L. M. Oleksa, G. M. Chisolm, and D. M. Driscoll.** 1995. Rat phospholipid-hydroperoxide glutathione peroxidase. cDNA cloning and identification of multiple transcription and translation start sites. J. Biol. Chem. **270:**26993–26999.
26. **Rousseaux, J., and R. Rousseaux-Prevost.** 1995. Molecular localization of free thiols in human sperm chromatin. Biol. Reprod. **52:**1066–1072.
27. **Roveri, A., M. Maiorino, and F. Ursini.** 1994. Enzymatic and immunological measurements of soluble and membrane-bound phospholipid-hydroperoxide glutathione peroxidase. Methods Enzymol. **233:**202–212.
28. **Roveri, A., F. Ursini, L. Flohe, and M. Maiorino.** 2001. PHGPx and spermatogenesis. Biofactors **14:**213–222.

28a. **Sega, G. A., R. P. Alcota, C. P. Tancongco, and P. A. Brimer.** 1989. Acrylamide binding to the DNA and protamine of spermiogenic stages in the mouse and its relationship to genetic damage. Mutat. Res. **216:**221–230.

29. **Shalgi, R., J. Seligman, and N. S. Kosower.** 1989. Dynamics of the thiol status of rat spermatozoa during maturation: analysis with the fluorescent labeling agent monobromobimane. Biol. Reprod. **40:**1037–1045.

29a. **Shelby, M. D., K. T. Cain, L. A. Hughes, P. W. Braden, and W. M. Generoso.** 1986. Dominant lethal effects of acrylamide in male mice. Mutat. Res. **173:**35–40.

30. **Shi, S. R., M. E. Key, and K. L. Kalra.** 1991. Antigen retrieval in formalin-fixed, paraffin-embedded tissues: an enhancement method for immunohistochemical staining based on microwave oven heating of tissue sections. J. Histochem. Cytochem. **39:**741–748.
31. **Ursini, F., S. Heim, M. Kiess, M. Maiorino, A. Roveri, J. Wissing, and L. Flohe.** 1999. Dual function of the selenoprotein PHGPx during sperm maturation. Science **285:**1393–1396.
32. **Ursini, F., M. Maiorino, R. Brigelius-Flohe, K. D. Aumann, A. Roveri, D. Schomburg, and L. Flohe.** 1995. Diversity of glutathione peroxidases. Methods Enzymol. **252:**38–53.
33. **Ursini, F., M. Maiorino, M. Valente, L. Ferri, and C. Gregolin.** 1982. Purification from pig liver of a protein which protects liposomes and biomembranes from peroxidative degradation and exhibits glutathione peroxidase activity on phosphatidylcholine hydroperoxides. Biochim. Biophys. Acta **710:**197–211.
34. **Watanabe, T., and A. Endo.** 1991. Effects of selenium deficiency on sperm morphology and spermatocyte chromosomes in mice. Mutat. Res. **262:**93–99.
35. **Weis, K.** 1998. Importins and exportins: how to get in and out of the nucleus. Trends Biochem. Sci. **23:**185–189.
36. **Yant, L. J., Q. Ran, L. Rao, H. Van Remmen, T. Shibatani, J. G. Belter, L. Motta, A. Richardson, and T. A. Prolla.** 2003. The selenoprotein GPX4 is essential for mouse development and protects from radiation and oxidative damage insults. Free Radic. Biol. Med. **34:**496–502.